





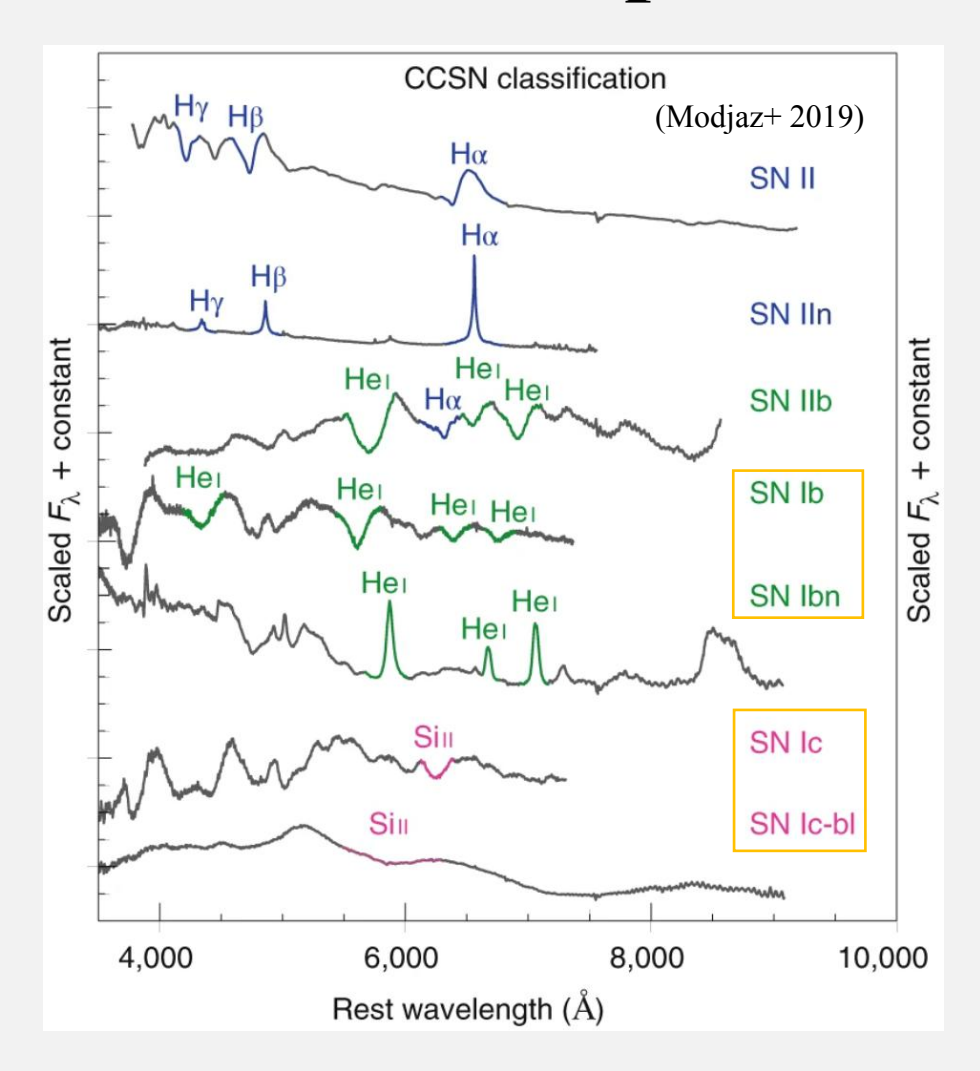
SN 2024iss: A double-peaked Type IIb Supernova with Evidence of Circumstellar Interaction

Liyang Chen et al. 2025

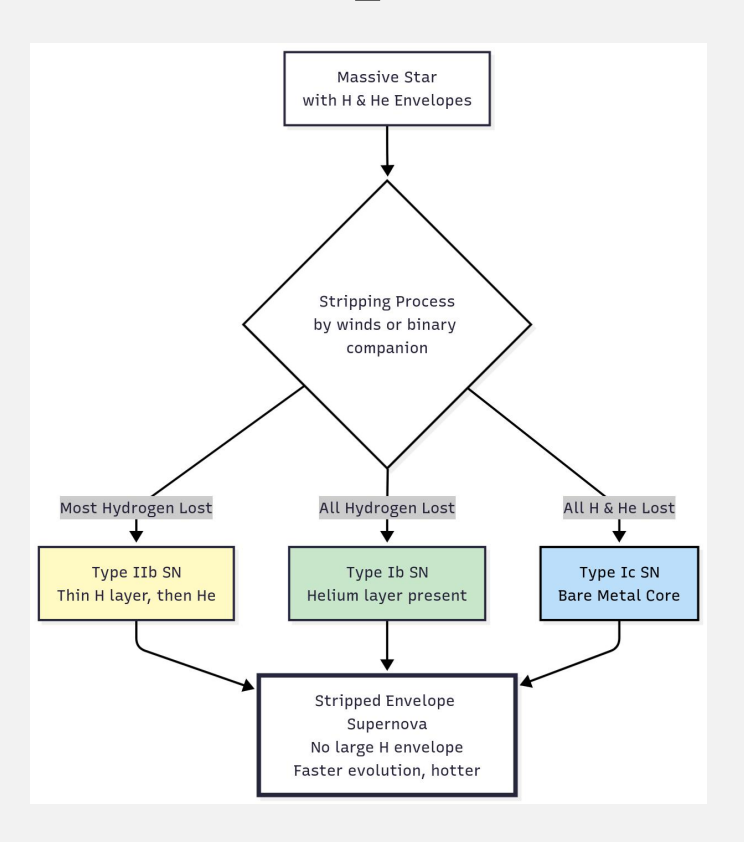
(ArXiv: 2510.22997v1)

Brajesh Kumar

Core-collapse SNe (Stripped Envelope SNe)



Spectroscopic features



- The mechanism stripping the envelopes of the progenitor star remains uncertain.
- Mainly **two channels**: single-star or binary interaction driven mechanisms.
- In the framework of wind-driven mass loss (single massive star) the stripping of a star can be intense and may indicate a massive progenitor such as a Wolf-Rayet star.

A explosion channel

Explosion of a massive star in a binary system:

- (1) Two stars orbit each other and draw closer and closer together.
- (2) The more massive star evolves faster, swelling up to become a supergiant. In this late phase of life, it spills most of its hydrogen envelope into the gravitational field of its companion star. As the companion siphons off almost all of the doomed star's hydrogen, it creates an instability in the primary star.
- (3) The primary star explodes in a supernova.
- (4) As the supernova fades, the surviving companion becomes visible (in a few cased with HST). The faint remnant of the supernova (lower left), continues to evolve (but not visible).

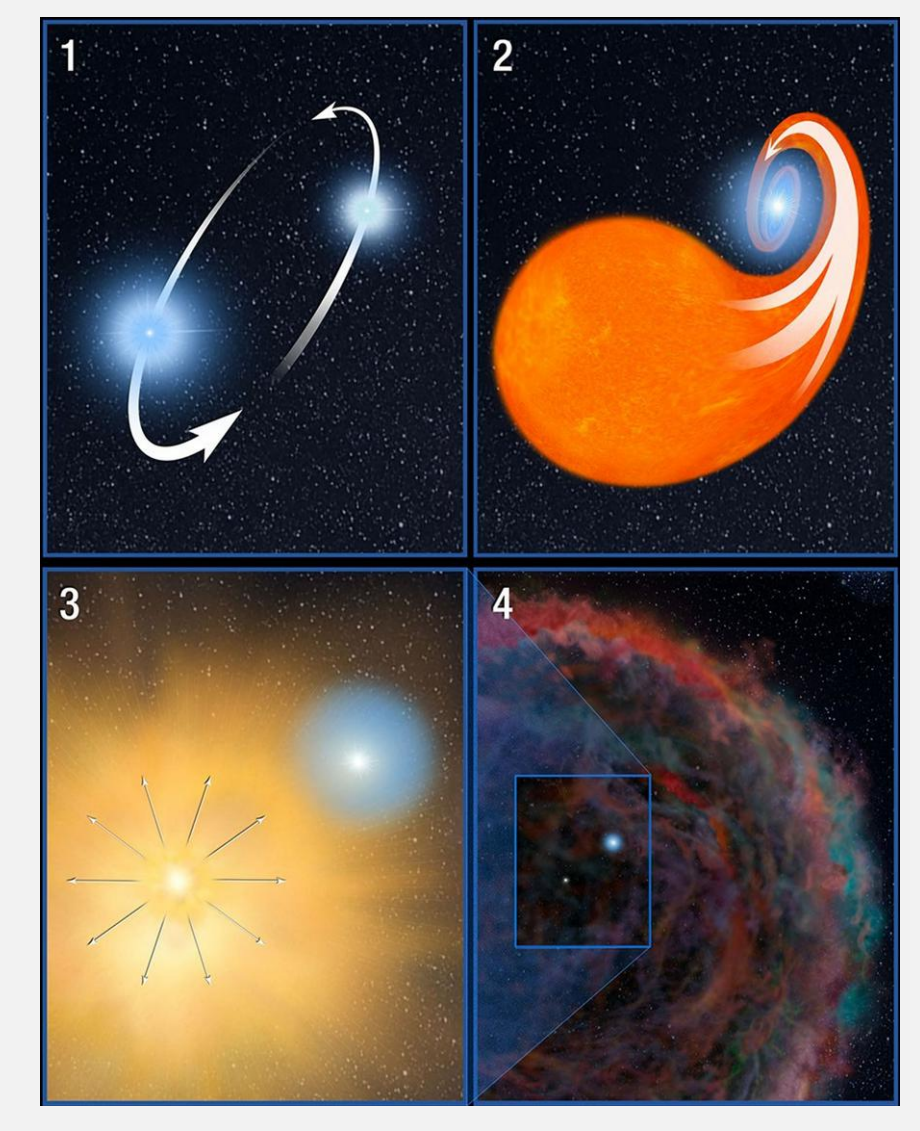
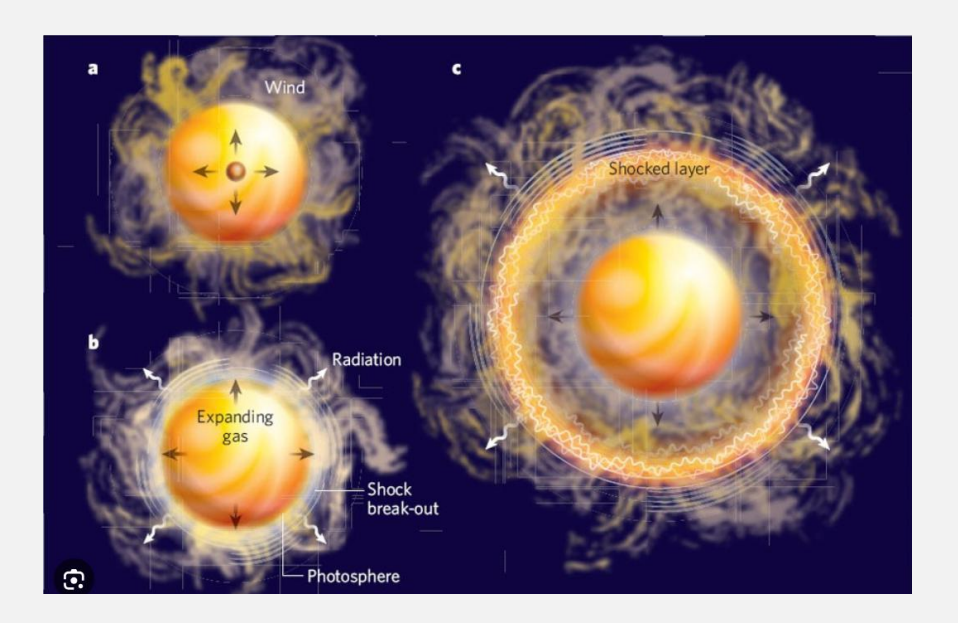


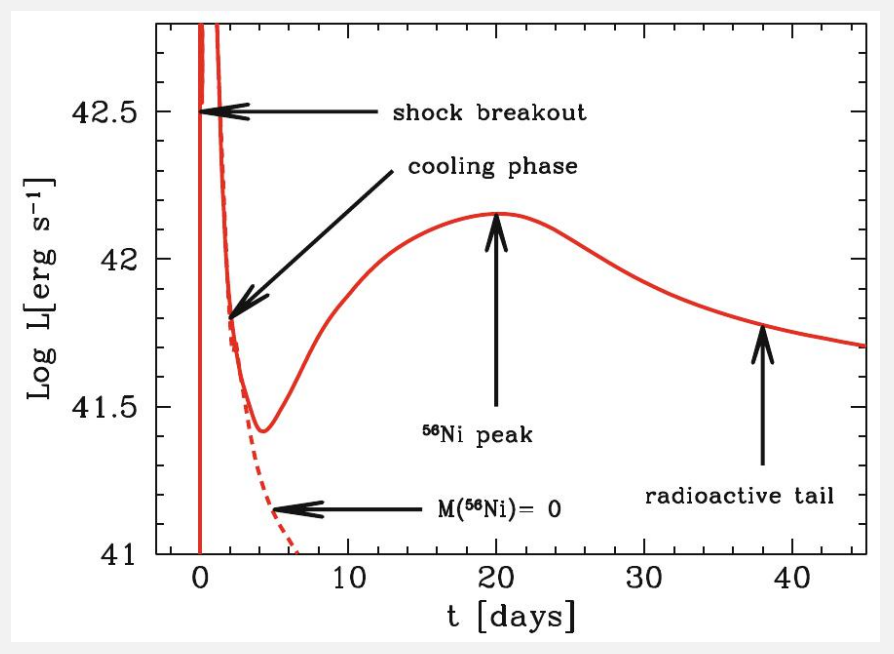
Image credit: NASA (SN 2001ig)

SE-SN Light curve

- In core-collapse supernovae (CC-SNe), when the shock generated by the gravitational collapse of core reaches the surface of the star (Shock Break Out), it results in a flash for a short duration.
- After SBO, the bulk of the exploded star expands and the effective temperature drops resulting in the cooling of the outermost layers (shock cooling phase).

- The LC of a normal SN I is powered by the shock energy (or explosion energy) and the radioactive decay (mainly of ⁵⁶Ni that is synthesized during the explosion).
- Main peak and beyond, radioactive decay: $^{56}\text{Ni} \rightarrow ^{56}\text{Co} \rightarrow ^{56}\text{Fe}$
- The expanding ejecta becomes optically thin during nebular phase.





X-ray emission from SNe

- The first SN to be discovered in X-rays was SN 1980K.
- The rapidly expanding high-velocity shock wave heats up the ambient medium to high temperatures, leading to copious amounts of thermal X-ray emission via thermal bremsstrahlung.
- Owing to pre-explosion mass loss and partial envelope stripping, some SNe IIb also exhibit signatures of circumstellar material (CSM), offering valuable insights into pre-explosion mass-loss history of their progenitor systems (Smith 2017).
- X-ray emission provides important trace of the ejecta-CSM interaction.
- Fransson et al. (1996) analyzed the X-ray emission of SN 1993J and attributed it to the thermal bremsstrahlung produced by the forward shock. This frame-work was extended in studies of SNe 2011dh (Soderberg et al. 2012) and 2013df (Kamble et al. 2016), further supporting the role of X-ray observations in providing critical constraints on the electron number density of the CSM around Type IIb SNe.

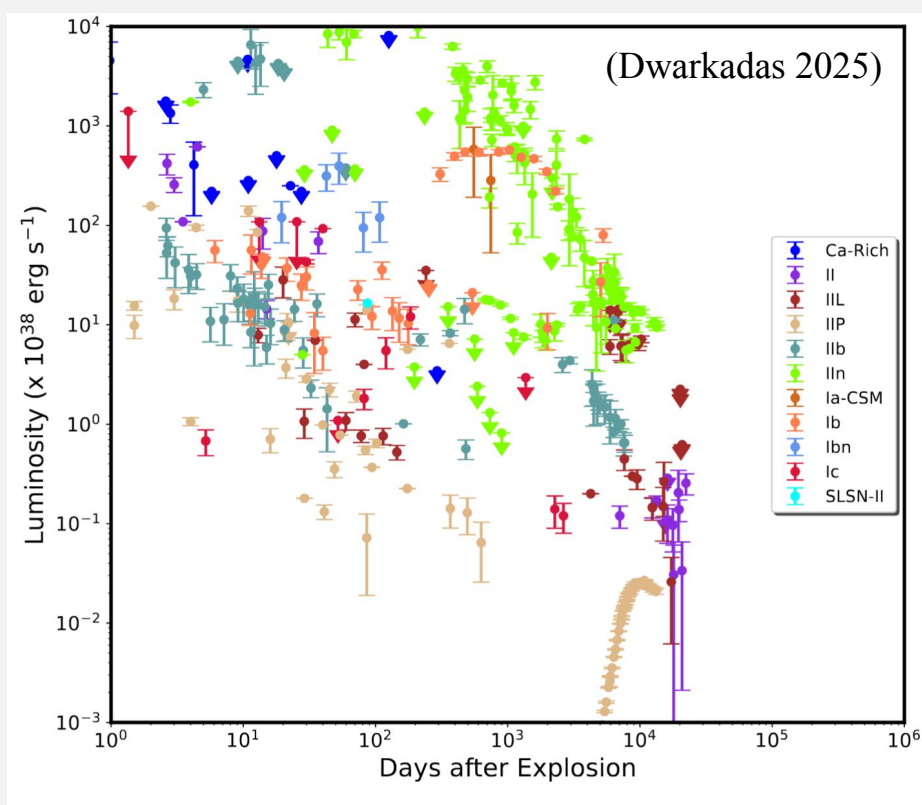
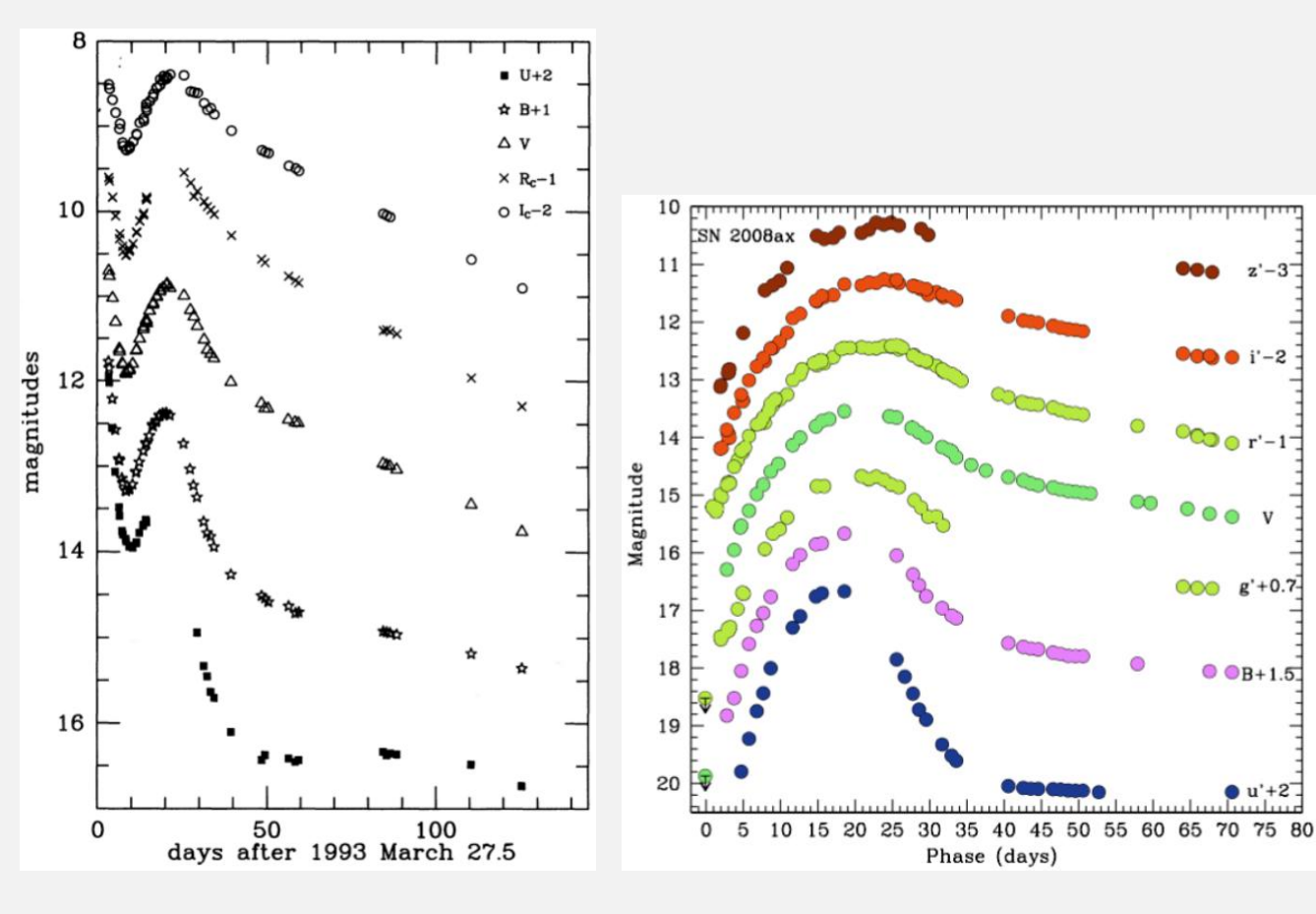


Figure 5. X-Ray Lightcurves of X-Ray SNe with at least one detection, grouped by type. SNe that were not detected but have upper limits are plotted with a downward facing arrow.

Extended (eIIb) and compact (cIIb)

- Chevalier & Soderberg (2010) classify **SNe IIb** into two subtypes (eIIb, cIIb) based on the prominence of their shock cooling emission.
- The extended subtype (Type eIIb) exhibits a pronounced shock-cooling peak in the early light curve, indicating a relatively massive hydrogen envelope ($\geq 0.1 \, \mathrm{M}_{\odot}$) and a large progenitor radius ($\sim 100-1000 \, \mathrm{R}_{\odot}$). These events typically show thermal X-ray emission and are surrounded by denser CSM.
- In contrast, objects belonging to the compact subtype (Type cIIb) display a weaker or no signature of shock cooling, indicating smaller sizes of their progenitors.
- The sample size of SNe IIb is still limited, and events with comprehensive optical and X-ray observations are even sparse. Further studies of the relationship between the envelope and the CSM will require a larger, well-characterized sample.



SN 1993J (Lewis+1994) Strong shock cooling (eIIb)

SN 2008ax (Pastorello+ 2008) No clear evidence of shock cooling (cIIb)

IIb SNe progenitor properties

• Mass range: $12-25 M_{\odot}$

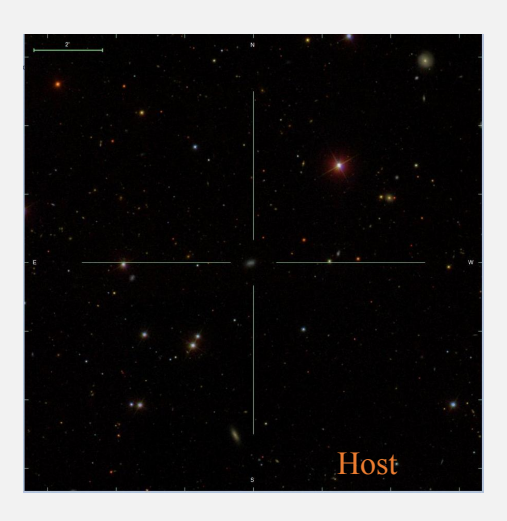
• Core mass range: $3-8~M_{\odot}$

- Only a thin layer of hydrogen ($< 0.5 M_{\odot}$) remains at the time of explosion.
- One way to investigate the nature of Type IIb SNe can be facilitated by analyzing the archival pre-explosion images. By fitting stellar evolutionary tracks to the spectral energy distribution (SED) extracted at the exact location of the SN on the archival images taken by the **Hubble Space Telescope (HST)**.

Example: SNe 1993J (Maund et al. 2004), 2013df (Van Dyk et al. 2014), 2016gkg (Kilpatrick et al. 2017; Tartaglia et al. 2017), 2017gkk (Niu et al. 2024) and 2024abfo (Reguitti et al. 2025; Niu et al. 2025).

• A more general approach to investigate the nature of the progenitor can be achieved by fitting the early-time emissions of the SN explosion with shock-cooling models. This process characterizes the energy emitted by the shock breakout deposited in the ejecta and describes how such energy diffuses out as the ejecta expands and cools.

SN 2024iss discovery and observations





Host galaxy	WISEA J125906.48+284842.6
RA (J2000)	$12^h 59^m 06.^s 130$
DEC (J2000)	+28°48′42.″62
Distance	$13.4 \pm 1.6 \text{ Mpc}$
Distance modulus	30.64 ± 0.26 mag
Redshift	0.003334
E(B-V) _{MW}	$0.0084 \pm 0.0002 \text{ mag}$
E(B-V)host	0.0
Explosion time	MJD $60442.21 \pm 0.44 (2024/05/12)$
V_{max}	MJD 60460.63 (2024/05/30)

- SN 2024iss was discovered on UT **2024 May 12 21:37** (MJD 60442.901) by the Gravitational-wave Optical Transient Observer (GOTO).
- ~Six hours before the reported discovery, the SN emission was recorded by outreach telescope located at the Xinglong Observatory.

Photometric Follow-up (UBgVrRIz bands, ~1-100 days after explosion):

- 0.36 m reflector of the Tsinghua University
- 0.8 m Tsinghua University-NAOC telescope
- 1.0 m Nanshan Wide-field Telescope
- 2.4 m Lijiang telescope of YNAO
- Schmidt 67/91 cm Telescope (67/91-ST)
- Copernico 1.82 m telescope at the Asiago Astrophysical Observatory
- Las Cumbres Observatory's global network of robotic telescopes (LCO)
- 3.58 m Telescopio Nazionale Galileo at La Palma and

Swift UVOT

• uvw1, uvw2, uvm2, u, b, and v bands

Optical Spectroscopy (51 epochs, ~1-87 days):

- B&C spectrograph on the 1.22 m Galileo Telescope
- FLOYDS spectrographs on 2 m Faulkes Telescopes South and North
- Beijing Faint Object Spectrograph and Camera on Xinglong 2.16 m telescope
- B&C spectrograph on University of Arizona's Bok 2.3 m
- Yunnan Faint Object Spectrograph Camera on Lijiang 2.4 m telescope
- Kast double spectrograph on Shane 3 m telescope at Lick Observatory
- DOLORES on the 3.5 m Telescopio Nazionale Galileo
- Binospec at the 6.5m MMT Observatory
- Gemini Multi-Object Spectrograph on 8.1m Gemini North Telescope
- Multi-Object Double Spectrographs on the 8.4 m Large Binocular Telescope
- Low Resolution Spectrograph 2 mounted on 10m Hobby-Eberly Telescope

X-ray Observations (Total 18 epochs between +2 to +34 days):

- Follow-up X-ray Telescope (FXT) on the Einstein Probe (EP)
- X-ray Telescope (XRT) on the Swift, and
- Nuclear Spectroscopic Telescope Array (NuSTAR)

SN 2024iss photometric evolution

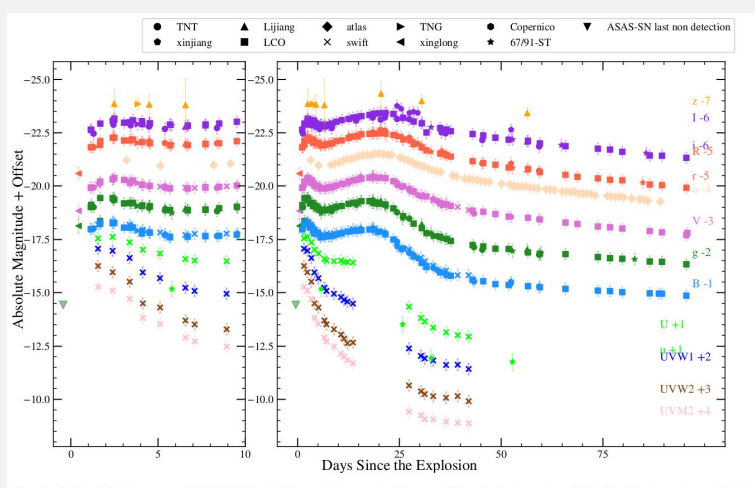


Fig. 1: Optical light curves of SN 2024iss. Left panel: the early-time multiband photometry within the first ten days. Right panel: the multiband light curves of SN 2024iss within the first \sim 100 days. All magnitudes were corrected for the Galactic extinction. For better display, light curves in different bandpasses were shifted vertically by arbitrary numbers as labeled on the right. Facilities used to obtain the photometry are indicated by the legend. The last non-detection from ASAS-SN is marked by the green inverted triangle.

- **(Fig.1)** Two phases: (1) early shock-cooling (from days 0 to 10 after the SN explosion), and (2) the later radioactive decay phases.
- SN 2024iss reached the first V-band peak of -17.33
 ± 0.26 mag on about day 2.4.
- Redder bands peak later than bluer ones. This evolution is consistent with the cooling of a hot blackbody, where the peak of the emission shifts progressively to longer wavelengths as the temperature decreases.

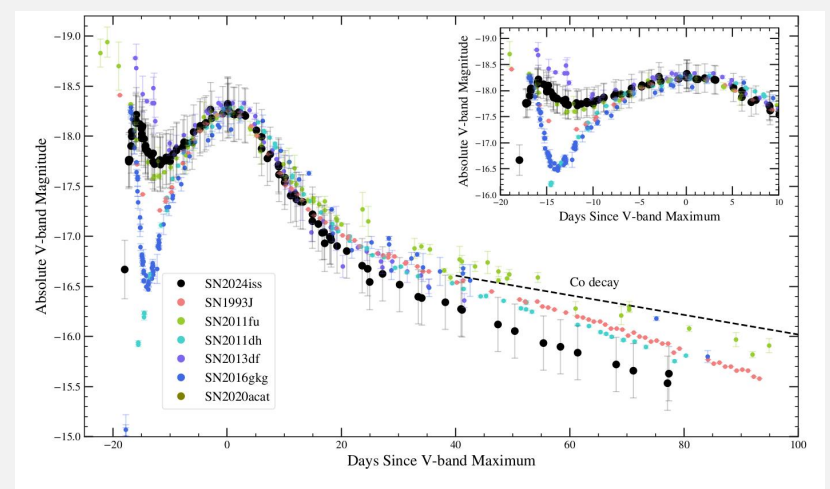


Fig. 2: The V-band light curve of SN 2024iss compared to those of well-sampled cases, i.e., the Type IIb SNe 1993J, 2011dh, 2013df, 2016gkg and 2020acat. The light curves of the comparison SNe have been shifted in both magnitude and time to align with the peak magnitude and the time of the V-band light curve peak of SN 2024iss. The black dashed line represents the expected decline rate of ⁵⁶Co (0.98 mag/100 day, [Woosley et al.] 1989). The upper-right inset shows a zoom-in of the first 30 days.

SN	Explosion Time	Time of the Second Peak	Redshift	m-M	$E(B-V)_{MW}$	$E(B-V)_{Host}$	Source ^a
	(MJD)	(MJD)		(mag)	(mag)	(mag)	
1993J	49074.0	49095.0	-0.001130	27.31	0.0690	0.110	1,2,3
2011dh	55712.0	55732.0	0.001638	29.46	0.0310	0.040	4
2011fu	55825.0	55846.9	0.001845	34.36	0.0680	0.150	5,6
2013df	56450.0	56469.0	0.002390	31.10	0.0170	0.081	7,8
2016gkg	57651.2	57669.0	0.004900	32.11	0.0166	0.090	9
2020acat	59192.0	59208.7	0.007932	32.74	0.0207	_	10

- (Fig.2) Beyond 50 days after the explosion, the light curves of SN 2024iss in all observed bandpasses enter a linear decline phase, with a characteristic V-band decline rate of ~2.0 mag/100 days (faster that the radioactive decay rate of ⁵⁶Co → ⁵⁶Fe, 0.98 mag/100 days). This indicates a faster evolution of SN 2024iss.
- SN 2024iss shows a prominent first peak, similar to that of SNe 1993J, 2011fu, 2013df and 2016gkg, but distinct from that of SNe 2011dh and 2020acat. Second peak has similarity with the compared IIb events.
- The prominent early peak of SN 2024iss indicates its extended-envelope nature.

Color evolution

- The U B color of SN 2024iss displays a continuous increase until setting to a plateau at a maximum of \sim 1.2 ± 0.37 mag at t \approx 35 days.
- The B V and g r colors show a similar evolution, with two distinct phases of increase of the color indices, which coincide with the first and second optical light curve peaks, respectively.
- From $t \approx 5$ to 20 days, both the B-V and g-r colors of SN 2024iss continue to become redder.
- Overall, such color evolution of SN 2024iss is broadly consistent with those of other SNe IIb, with the exception of SN 2011dh, which does not show a clear initial rapid reddening phase and only exhibits a very shallow initial decline in the V band.

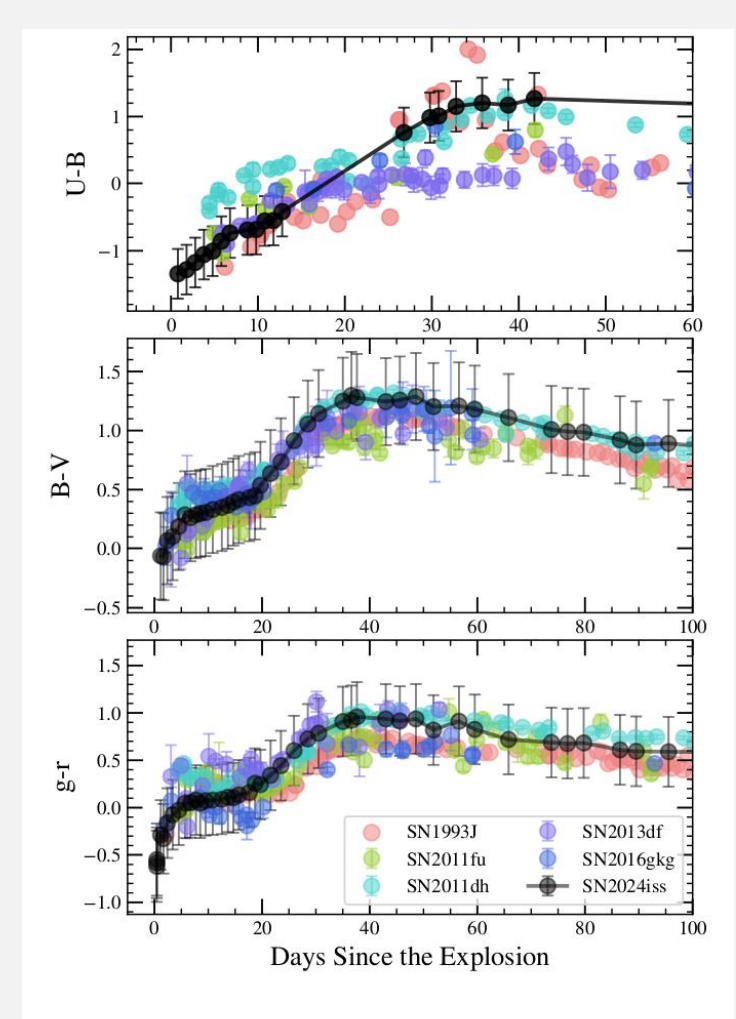


Fig. 3: Galactic reddening-corrected U-B, B-V, and g-r color curves of SN 2024iss, compared with Galactic reddening-corrected color curves of SNe 1993J, 2011fu, 2011dh, 2013df, and 2016gkg. For the purpose of display, the V-R color curve of SNe 1993J, 2011fu, 2013df and 2016gkg were converted to g-r using the transformation from Jordi et al. (2006).

Pseudo-bolometric Luminosity and Temperature evolution

- Light Curve Fitting package by Hosseinzadeh & Gomez (2020) was used to construct the pseudo-bolometric light curve of SN 2024iss. The UV, optical, and NIR (uvw2, uvm2, uvw1, B, V, g, r, i, J, H, and K-band) fluxes were integrated.
- The maximum pseudo-bolometric luminosity of SN 2024iss yields $L = (1.2 \pm 0.4) \times 10^{43}$ erg s⁻¹, on day 1.2.
- The pseudo-bolometric light curve subsequently declines until reaching a turning point on day 6.7. The light curve then rises again until a secondary peak of L = 3.1×10^{42} erg s⁻¹
- The pseudo-bolometric luminosity of SN 2024iss at its secondary peak is slightly above the mean peak luminosity of SNe IIb given by Prentice et al. (2016). This may result from either a larger amount of ⁵⁶Ni synthesized during the SN explosion or a more thorough mixing of ⁵⁶Ni in the ejecta (Liu et al. 2025).
- Both the temperature and photospheric radius of SN 2024iss show similar evolution to those of other SESNe.

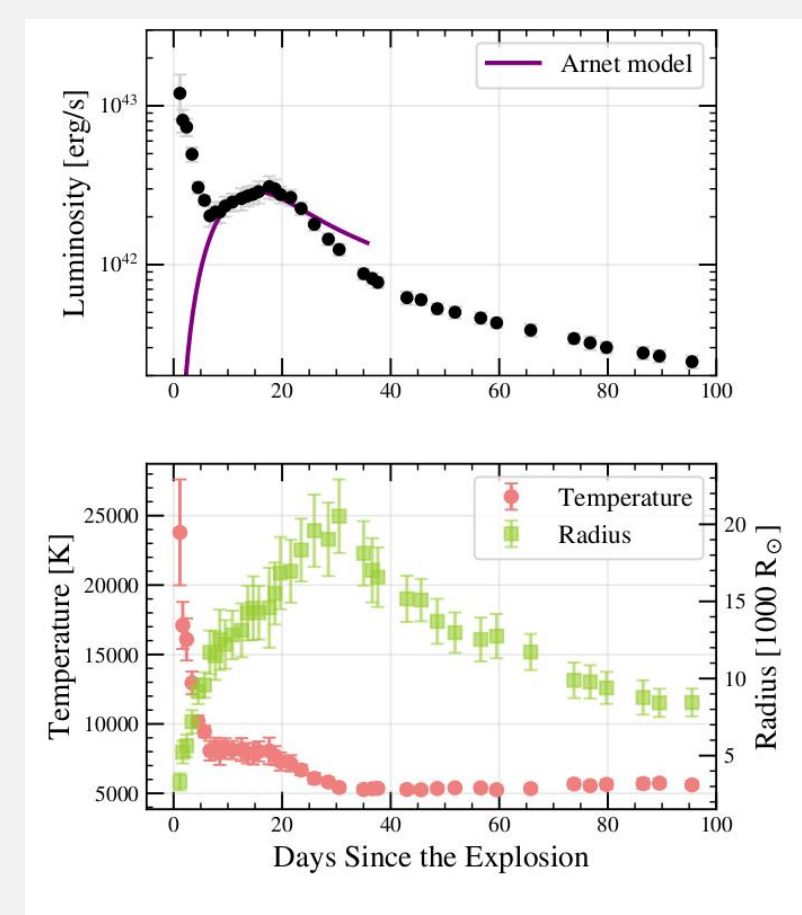


Fig. 4: Top: Pseudo-bolometric light curve of SN 2024iss. The purple line shows the best-fit Arnett model to the secondary peak. Bottom: Evolution of the blackbody temperature and the photospheric radius of SN 2024iss, as indicated by the left- and right-hand ordinates, respectively.

Explosion parameters

• The second peak of the BLC was fitted with the Arnett + Valenti models. This is an **oversimplified expanding fireball model to explain the early LC of Type Ia supernovae (SNe Ia) by Arnett (1982) and later** extended to SESNe (Valenti 2008) by separating their **photometric evolution into the photospheric and nebular phases, and introducing a γ-ray leakage term.**

$$\tau_m = \sqrt{2} \left(\frac{\kappa_{\rm opt}}{\beta c} \right)^{1/2} \left(\frac{M_{\rm ej}}{v_{\rm ph}} \right)^{1/2}$$

$$E_k \approx \frac{3}{5} \frac{M_{\rm ej} v_{\rm ph}^2}{2}$$

$$M_{ej}$$
 = Ejecta mass
 t_m = photon diffusion time
 k_{opt} = optical opecity
 v_{ph} = photospheric velocity
 β = constant(13.8)
 c = speed of light

- Considered phot velocity (v_{ph}) of 7500 km s⁻¹, (measured from absorption minimum of the Fe II λ 5169 in the near-maximum-light spectrum).
- The estimated parameters are
 - $M_{Ni} = 0.117 \pm 0.013 \text{ M}_{\odot}$
 - $M_{ej} = 1.272 \pm 0.343 \text{ M}_{\odot}$
 - $E_k = 0.427 \pm 0.115 \times 10^{51}$ erg.

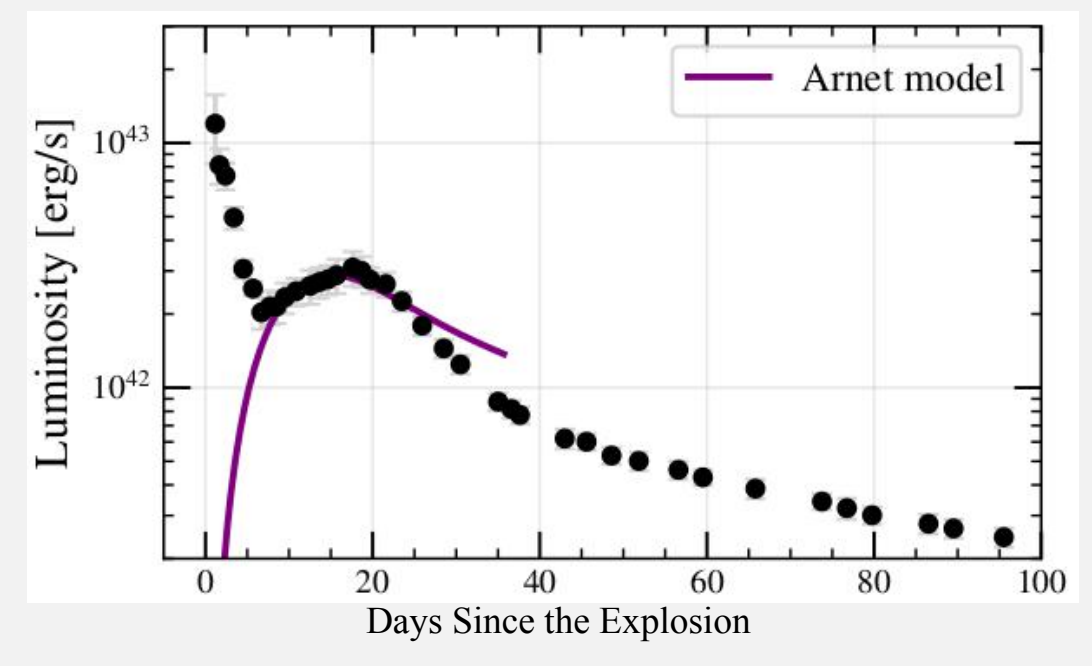


Fig. Best-fit Arnett model to the secondary peak.

Spectral evolution

(First 7 days)

- The spectra of SN 2024iss are characterized by **blue and featureless continuum**.
- At this stage, the SN emission is dominated by the shock cooling. The outermost envelope of the exploding progenitor star manifests sufficiently high temperature at the location of the photosphere, where the high opacity lineforming regions were not often present.
- Features of He I λ 5876, H γ and Ca II NIR $\lambda\lambda$ 8498, 8542, 8662 can be also identified in the spectra starting from t \approx 5.3 days.

(~8-87 days)

- He I λ 5876, 6678 features become progressively prominent after the shock cooling.
- As the ejecta cool, the [Ca II] $\lambda\lambda7291$, 7323 doublet appear around day 32, followed by a series of oxygen lines, i.e., [O I] $\lambda\lambda6300$, 6364 and O I $\lambda7774$. Such signatures can be clearly identified in the t \approx 61 day spectrum.
- By $t \approx 87$ days, as the ejecta cool, various **forbidden lines become prominent** in the spectrum, i.e., double peak in the Ca II $\lambda\lambda8498$, 8542, 8662 feature.

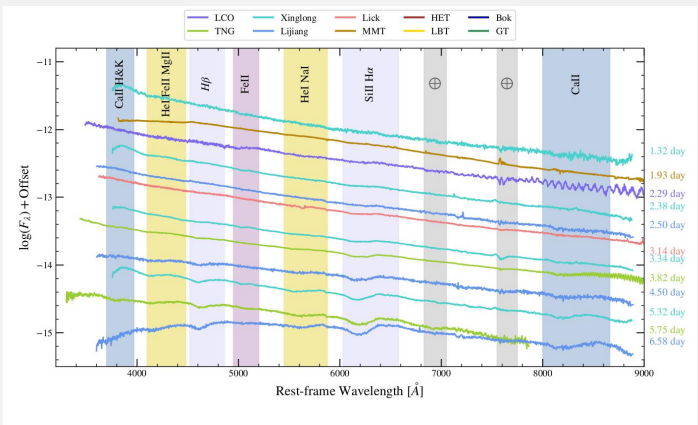


Fig. 5: Spectral sequence of SN 2024iss, spanning the first 7 days after the explosion. Phases are marked on the right. Different colors distinguish the different spectrographs used in the observations, as shown at the top. A log of the spectroscopy of SN 2024iss is given in Table [A.3]

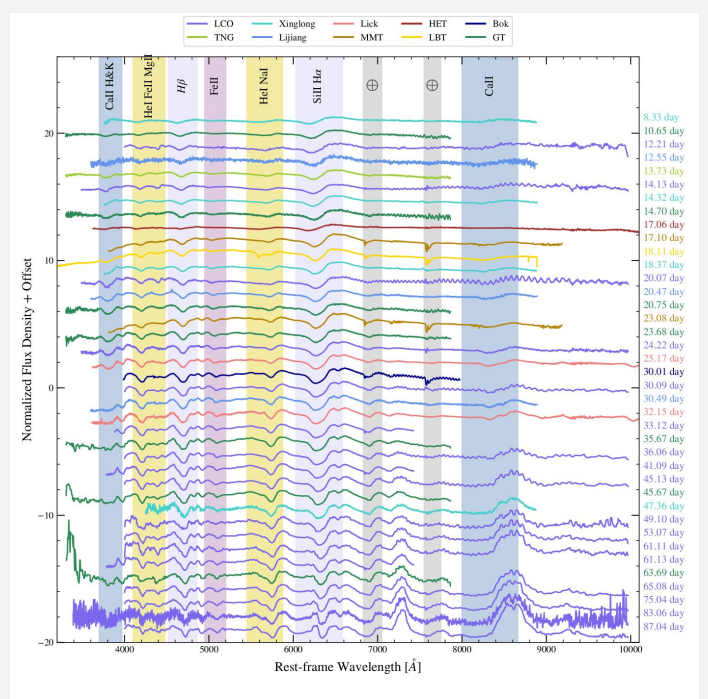


Fig. 6: Spectral consequence of SN 2024iss obtained during the phase from t≈ 8 to 87 days after the explosion. The layout of the figure is similar to those of Figure S For the purpose of presentation, the best-fit blackbody function was subtracted from each spectrum. A log of the spectroscopy of SN 2024iss is presented in Table [A.3]

Spectral comparison with other IIb events

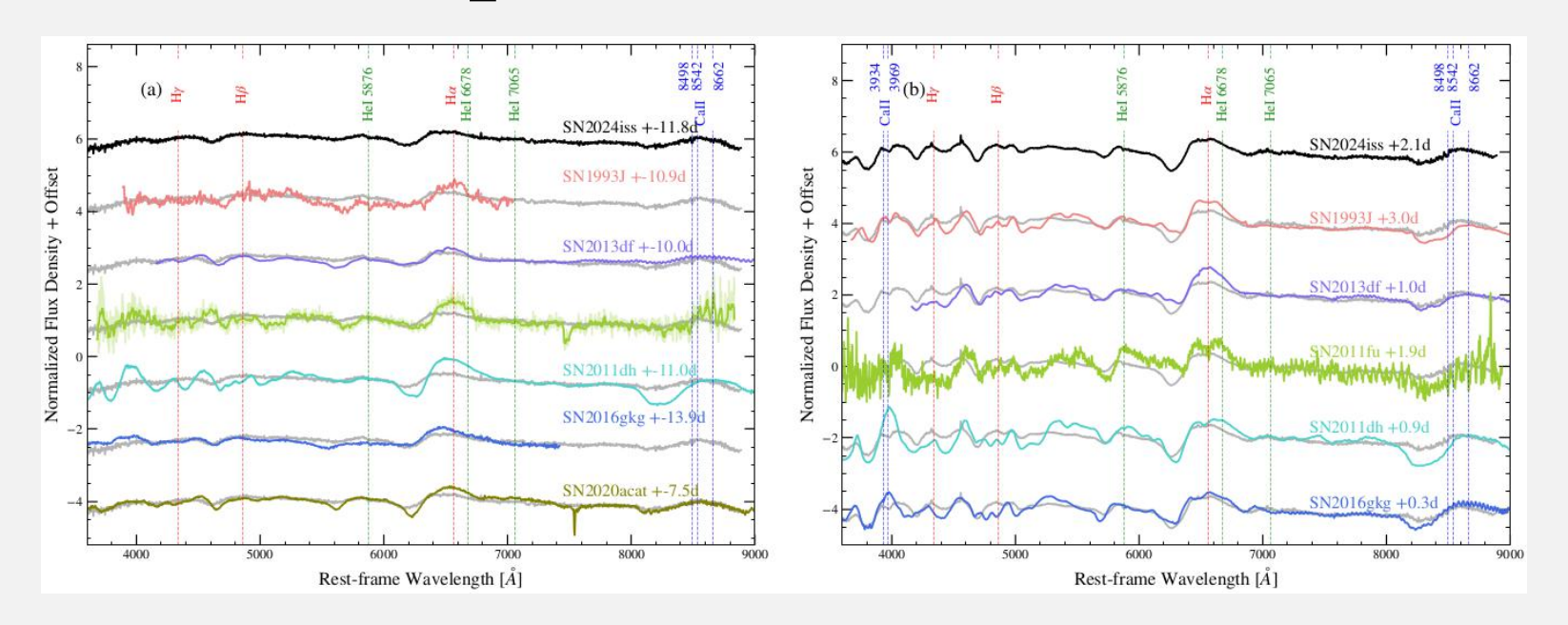


Fig. (a)

- At early phases (\sim -12 days), SNe 2024iss and 1993J exhibit similar H α and H β profiles, while SN 1993J displays a more prominent He I λ 5876.
- The Ca II NIR triplet profile of SN 2024iss shows a good resemblance to SN 2020acat.
- SNe 2011dh and 2011fu exhibit more prominent line profiles at about ten days before V-band maximum, indicating a prompt spectral evolution.

Fig. (b)

- At around the V-band maximum, SNe 2024iss and 1993J exhibit a flat-topped emission component of H α , which may likely be caused by the strengthening He I λ 6678.
- SN 2013df displays a single-peaked Hα emission, while SNe 2011dh and 2011fu exhibit double-peaked profiles, likely indicating a prompt mixing of helium into the H-rich envelope.
- SN 2011fu shows the most prominent He I λ 5876 feature among the sample.

Spectral comparison with other IIb events

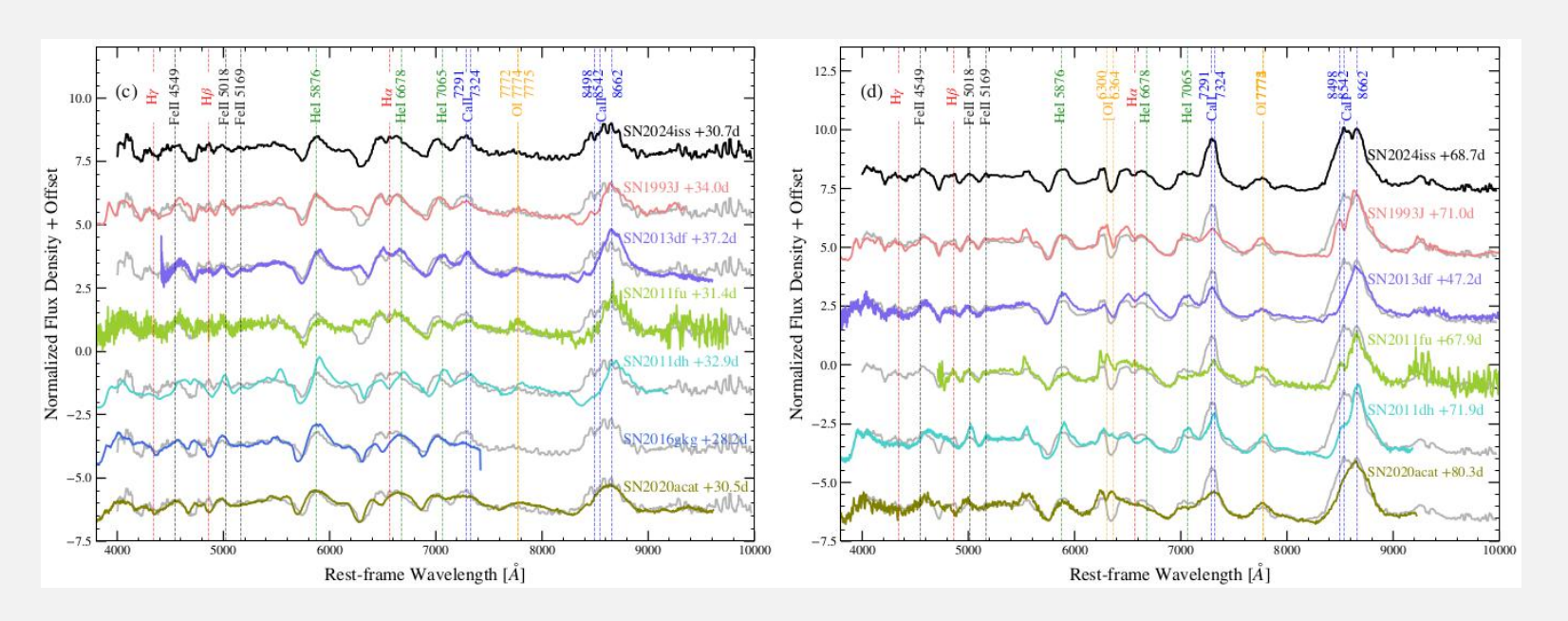


Fig. (c), spectra comparison ~30 days

- SN 2024iss exhibits broader Ca II λλ8498, 8542, 8662 absorption in comparison with other SNe.
- Furthermore, unlike the significantly weakened Hα absorption component observed in SNe 1993J and 2013df, such a feature still remains prominent in SNe 2024iss, 2016gkg, and 2020acat.

Fig. (d), Spectra comparison around 70 days

- The iron features became more prominent, indicating a transition to the nebular phase, when the continuum spectral emission becomes dominated by a blend of Fe-group features.
- The strength of the Balmer lines are decreasing while several He I lines remain strong, highlighting the type IIb nature of the SN.

Shock-Cooling Model Fitting

- Sapir & Waxman (2017) model was used to fit the multiband light curves of SN 2024iss up to $t \approx 5$ days after the explosion.
- The key parameters include the envelope radius (R), the envelope mass (M_{env}) , the shock velocity (v_s) , the product of stellar mass and a numerical factor related to envelope structure $(f\rho M)$ and the first-light time (t_0) .

Estimated fitting parameters:

R = 244 ± 43 R_{\odot} , $M_{\rm env}$ = 0.11 ± 0.04 M_{\odot} , $v_{s,8.5}$ = (1.9 ± 0.3) × 10^{8.5} cm s⁻¹, $f_{\rho}M$ = 100 ± 65 M_{\odot} and $t_{\rm exp}$ = 60442.41 ± 0.05 d. The model light curves agree fairly well with the observations. The inferred envelope mass and radius of SN 2024iss are larger than that of SN 2016gkg (i.e., ~0.03 M_{\odot} , ~141 R_{\odot} ; Piro et al. 2021), indicating a more extended envelope than Type cIIb SNe. The envelope mass of SN 2024iss is lower than that of SN 1993J (~0.2 M_{\odot} ; Woosley et al. 1994), suggesting that its envelope is less extended than some Type eIIb SNe.

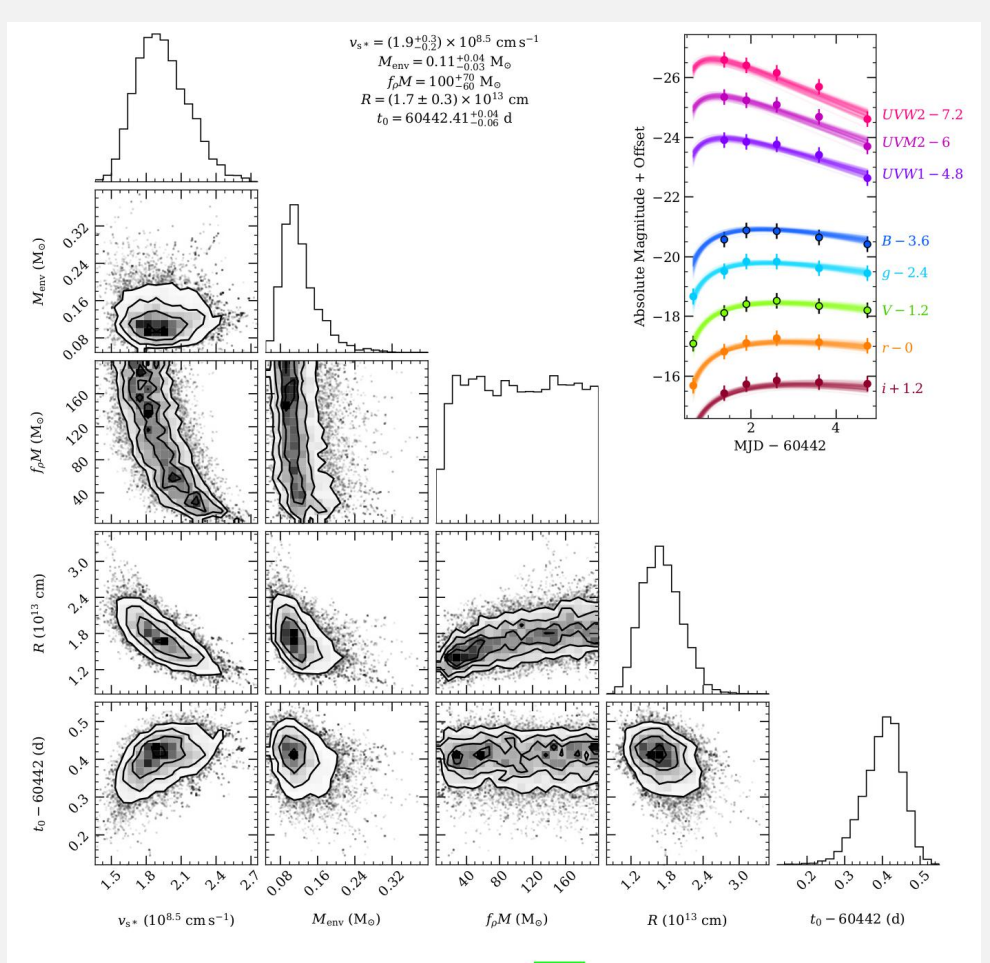


Fig. 10: The Corner plot that presents the posterior distributions of the SW17 shock-cooling light-curve model of SN 2024iss. The fit to the early light curves was restricted to five days after the estimated time of the SN explosion. The best-fit parameters are listed at the top of the figure. The upper-right inset presents the model light curves that best fit the multiband photometry, as displayed by color-coded curves and symbols, respectively.

X-ray Constraints on the Circumstellar Medium

Fig. 11: The mass-loss rate was constrained as 1.2-1.9 × 10^{-5} and $1.0-2.2 \times 10^{-5}$ M_☉ yr⁻¹, respectively for the 3σ and 5σ confidence intervals of the 3–10 keV luminosity.

The mass loss rate inferred for SN 2024iss is comparable to SNe 1993J and 2013df.

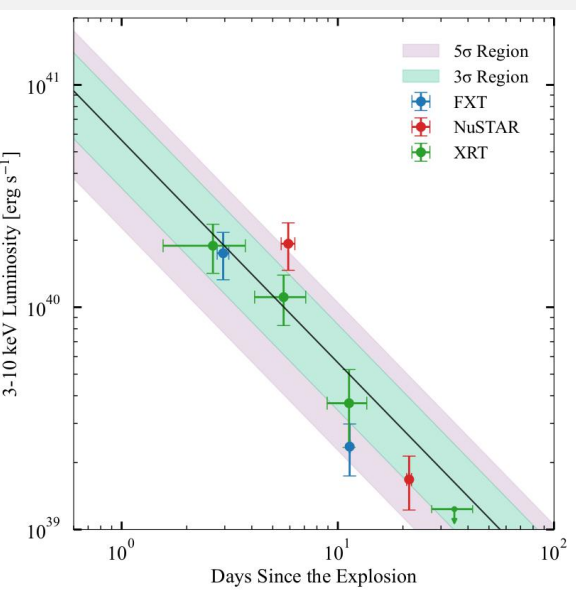


Fig. 11: The unabsorbed X-ray luminosity of SN 2024iss observed in the 3–10 keV band. The red, green, and blue data points represent the observations conducted with the NuSTAR, Swift-XRT, and EP-FXT, respectively. The black line shows the best-fit thermal bremsstrahlung model, with a mass-loss rate of $1.6 \times 10^{-5} \ M_{\odot} \ yr^{-1}$ and a shock velocity of $9.5 \times 10^8 \ cm \ s^{-1}$. The green and purple shaded areas indicate the $3-\sigma$ and $5-\sigma$ confidence regions, respectively.

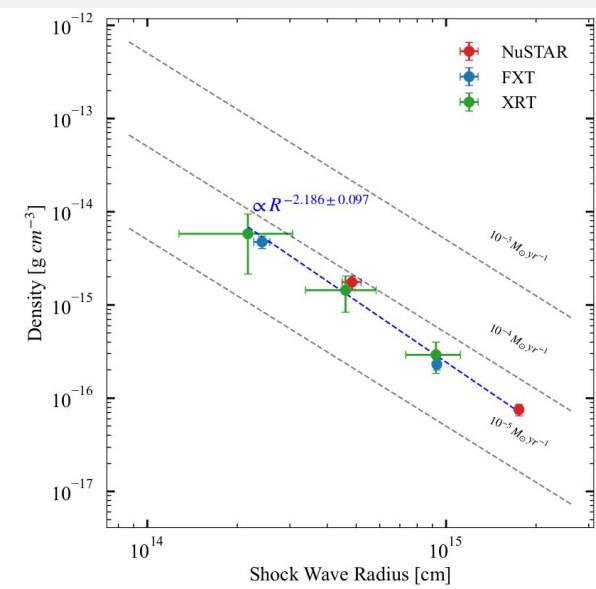


Fig. 12: The CSM density profile as inferred from the emission measure. Data from NuSTAR, Swift-XRT, and EP-FXT are indicated by the red, green, and blue circles, respectively. The gray dashed lines represent the wind-like density profiles corresponding to mass-loss rates of $\dot{M}=10^{-5},\ 10^{-4},\ 10^{-3}\ M_{\odot}\ yr^{-1}$. The blue dashed line denotes the power-law fit to the X-ray light curve. The inferred radial density profile $\rho_{\rm CSM} \propto R^{-2.19}$ is incompatible with a homogeneous mass-loss wind.

Fig. 12: shows the radial density profile of the CSM around SN 2024iss (ρ_{CSM}) as inferred from the emission measure method, together with homogeneous wind with different massloss rates. The former lies between the 10^{-5} and 10^{-4} M_{\odot} yr⁻¹ curves of steady mass loss, with a mean value of $(5.55 \pm 1.57) \times$ $10^{-5} \,\mathrm{M}_{\odot} \,\mathrm{yr}^{-1}$.

Discussions

SN 2024iss Progenitor:

- The best fit to the Arnett model based on the second light curve peak of SN 2024iss suggests an ejecta mass of $M_{ej} = 1.27 \pm 0.34 \,\mathrm{M}_{\odot}$. Assuming a typical mass for the neutron star remnant of 1.4 M_{\odot} (Thorsett & Chakrabarty 1999), they estimate a helium core mass of $M_{remnant} + M_{ej} + M_{env} = 2.8 \,\mathrm{M}_{\odot}$.
- Using the progenitor grid of Sukhbold et al. (2016), this indicates a main-sequence mass of $M_{ZAMS} = 9 11 M_{\odot}$, which is similar to that inferred for SN 2016gkg.
- They estimate the mass and radius of the hydrogen envelope of SN 2024iss as $M_{env} = 0.11 \pm 0.04 \ M_{\odot}$ and $R_{env} = 224 \pm 43 \ R_{\odot}$. The inferred mass and radius favors for a YSG progenitor star. A binary system may naturally account for the partially depleted hydrogen envelope required for the progenitor of SN 2024iss.

SN 2024iss: Bridging the Gap between subclasses of Type eIIb and Type cIIb

- The envelope mass of SN 2024iss is close to the threshold of 0.15 M_{\odot} adopted to distinguish between Types eIIb and cIIb.
- For comparison, the compact Type IIb SN 2016gkg has an envelope mass of ~0.03 M_{\odot} , while the extended Type IIb SN 1993J exhibits a much larger envelope mass of ~0.2 M_{\odot} . Similarly, the envelope radius of SN 2024iss is larger than that of the compact SN 2008ax (~40 R_{\odot}), but smaller than that of SN 1993J (~575 R_{\odot}).
- The envelope properties emission suggest that SN 2024iss likely represents a transitional object lying between the compact and extended subtypes of Type IIb SNe.

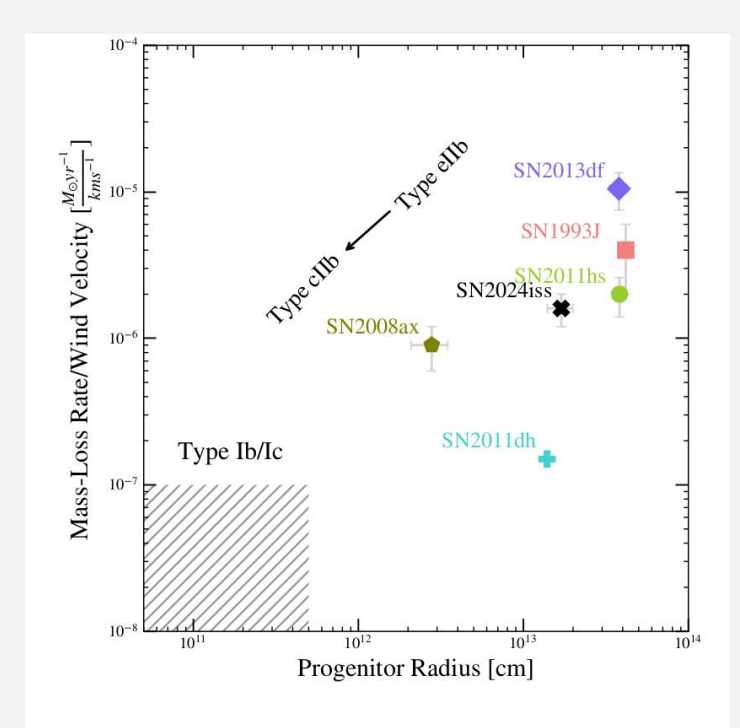


Fig. 14: Comparison between the mass-loss rate normalized by wind velocity $(\dot{M}/\nu_{\rm w})$ and the progenitor radius. The shaded region indicates typical CSM densities of Type Ib/c SNe(Chevalier & Fransson | 2006), though these estimates may suffer from systematic uncertainties of up to an order of magnitude (Maeda et al. | 2012). Color-coded symbols represent the estimated values for different SNe as labeled. The upper-right to lower-left arrow illustrates a possible evolutionary sequence from Type eIIb to cIIb and eventually to Type Ib/Ic SNe.

More extended progenitors tend to have experienced a stronger mass loss.

Discussions

Implications of the Low Ejecta Mass of SN 2024iss

- The Arnett model fit to the bolometric light curve of SN 2024iss suggests an ejecta mass of $1.27\pm0.34~M_{\odot}$ and a ^{56}Ni mass of $0.117\pm0.013~M_{\odot}$. While the Ni mass is consistent with the average value derived for SNe IIb, the ejecta mass of SN 2024iss is lower than ejecta masses of SNe 1993J, 2011dh, and 2013df (~2-3.5 M_{\odot}).
- It appears to be a faster decliner as indicated by its Δm_{15} (V) = 1.13 mag, compared to the mean value of 0.93 mag inferred for SNe IIb (Taddia et al. 2018). The late-time decay rate also approaches 2 mag per 100 days, one of the steepest in the sample.
- Objects with higher $E_K/M_{\rm ej}$ ratios are less efficient in trapping gamma-rays, and therefore exhibit a steeper late-time decline and a narrower light-curve peak.
- Prentice et al. (2018) found that the ejecta masses of SNe IIb exhibited a bimodal distribution (peaking at 1.9 and 3.9 M_{\odot}). Such a bimodal mass distribution of the ejecta may indicate a discontinuity of the intrinsic properties of Type IIb SNe with one group having more extended and the other having a rather compact envelope. The ejecta mass of SN 2024iss falls within the lower ejecta mass regime, consistent with its Type eIIb classification.

X-ray investigation of SN 2024iss: a confined structure of CSM

Summary

- The optical light curves of SN 2024iss exhibit a double-peak feature. The first V-band peak, which can be attributed to shock cooling, occurred at ~2.4 days after the explosion and reached a peak magnitude of $M_V = -17.33 \pm 0.26$. The second peak, powered by ⁵⁶Ni decay, reached a peak magnitude of $M_V = -17.43 \pm 0.26$ at ~18.7 days after the SN explosion.
- The best-fitting parameters are $M_{Ni} = 0.117 \pm 0.013 \ M_{\odot}$, $M_{ej} = 1.272 \pm 0.343 \ M_{\odot}$ and $E_k = 0.427 \pm 0.115 \times 10^{51}$ erg. The inferred ⁵⁶Ni mass is typical for Type IIb SNe, while the relatively low ejecta mass is compatible with the rapid decline in luminosity, as indicated by the large Δm_{15} value of 1.13 mag, compared to an average of 0.93 mag for Type IIb SNe.
- The best-fit (shock-cooling) parameters are: $R_{env} = 244 \pm 43 R_{\odot}$, $M_{env} = 0.11 \pm 0.04 M_{\odot}$, and $v_s = (1.67 \pm 0.07) \times 10^4 \text{ km s}^{-1}$.
- SN 2024iss exhibits bright thermal bremsstrahlung emission from the forward shock. The strength of the emission is comparable to that observed in SNe 1993J and 2013df. X-ray analysis indicates a significant mass ejection may have occurred within about four years prior to the SN explosion.